Available online at www.sciencedirect.com

ScienceDirect

Energy Procedia 69 (2015) 1220 – 1230

Energy Procedia

International Conference on Concentrating Solar Power and Chemical Energy Systems, SolarPACES 2014

Power block off-design control strategies for indirect solar ORC cycles

D. Casartelli[a], M. Binotti[a]*, P. Silva[a], E. Macchi[a], E. Roccaro[b], T. Passera[b]

[a]*Politecnico di Milano, Dipartimento di Energia, Via Lambruschini 4, 20156 Milano, Italy*
[b]*Centro Ricerche per le Energie Non Convenzionali – Istituto Donegani. Via Fauser 4, 28100 Novara, Italy*

Abstract

The performance of a $5MW_{el}$ indirect ORC cycle coupled to linear solar collectors with different technologies is assessed, aiming at evaluating the effect of different control strategies on annual electricity output. Two different solutions are considered for solar collectors: a state-of-the-art parabolic trough collector with Therminol VP1 as heat transfer fluid (HTF), reaching 390°C as maximum temperature within the solar field, and a cheaper Linear Fresnel Reflector (LFR) with Therminol 55, limited to an operating temperature of 310°C. A simplified procedure is firstly proposed in order to identify the organic fluid that guarantees the highest performance under design conditions. Toluene is the selected working fluid in a saturated regenerative Rankine cycle configuration. After fluid selection, a more detailed analysis involving turbine sizing and piping estimate is carried on in order to set optimal on-design parameters such as the evaporating pressure of the working fluid. Finally, yearly electricity production is calculated taking into account off-design performance of all plant components as a function of the effective solar radiation. Two different off-design control strategies are considered for the turbine, namely sliding pressure and constant pressure at the turbine inlet. The levelized cost of electricity (LCOE) is computed for both cases. For high temperature collectors the LCOE results respectively about 180 €/MWh with partial admission and 175 €/MWh with sliding pressure off-design control strategy. LFR technology leads to similar LCOE when its specific cost is about half than the parabolic trough collector.

Peer review by the scientific conference committee of SolarPACES 2014 under responsibility of PSE AG

*Keywords:*Small scale CSP; solar ORC; ORC cycle; Turbine control strategy

* Corresponding author. Tel.: +39-02-2399-3935; fax: +39-02-2399-3913.
E-mail address: marco.binotti@polimi.it

Peer review by the scientific conference committee of SolarPACES 2014 under responsibility of PSE AG
doi:10.1016/j.egypro.2015.03.166

1. Introduction

Organic Rankine Cycles (ORC) are typical power cycles adopted either for low temperature heat sources, or for medium-high temperature heat sources and relatively low thermal power inputs. ORC can be considered a consolidated and reliable technology that offers relatively high efficiency, simple start up and O&M procedures, and proven long life. They have been widely adopted for many years for geothermal reservoir exploitation [1], biomass applications [2] or bottoming cycles and industrial waste heat recovery [3, 4]. Solar-ORC plants can be competitive from an economic point of view in the range of few MW [5]. Commercial ORC-based CSP plants went recently on-line [6], and new ones are in the project or are currently under construction. Besides the well known benefits of distributed generation, another potential advantage of solar ORC cycles is the possibility of cogenerating electricity and useful heat for very high energy efficiency and flexibility.

In the present paper the performance of a non-cogenerative $5MW_{el}$ ORC cycle coupled with two types of linear collectors in the solar field (SF) is considered. The solar collectors are respectively a state-of-the-art parabolic trough collector with synthetic oil Therminol VP1 as HTF and a maximum temperature of 390°C, and a cheaper Linear Fresnel Reflector (LFR) with Therminol 55, limited to an operating temperature of 310°C. In both cases Toluene is the selected working fluid in a saturated regenerative Rankine cycle. Turbine sizing is performed with an in-house code and two different off-design control strategies are compared for the plant, respectively sliding pressure and a fixed pressure at the turbine inlet. The first one is easy to implement in an actual plant and leads to a reliable operation, while the latter gives some advantages by the point of view of efficiency. The aim of the paper is to investigate the effects of the selected control strategies on electricity production during part-load operation. The off-design behavior of each component is studied and the entire system off-design performance as a function of the effective solar radiation is computed. Yearly simulations are then performed for a specific site and the LCOE is finally computed for both operating strategies and both collectors. Future works will deal with superheated ORC cycles and thermal storage systems to increase the electricity dispatching, as well as with cogenerative applications.

2. Methodology

The solar plant type is a 5 MW gross power output system with linear collectors, synthetic oil as HTF and without thermal storage. Two different solutions are investigated for the solar field: the use of standard parabolic trough ET-100 [7] collectors with Therminol VP1 [8] as HTF (called HT solution) or the use of cheaper collectors (Soltigua Linear Fresnel Reflector [9]) with Therminol 55 [10] and limited maximum temperature (called LT solution). The solar multiple is set equal to 1.2 (800 W/m^2 DNI) as proposed in [11]. The adopted ORC cycle is a saturated regenerative ORC cycle with no superheating and a wet cooling tower condensing system. The plant layout is reported in Fig. 1, together with an example of cycle T-s diagram with Toluene as working fluid. The cycle and plant performances are computed using Excel®, VBA and REFPROP® [12], initially assuming a series of simplifications on turbine and solar field performances.

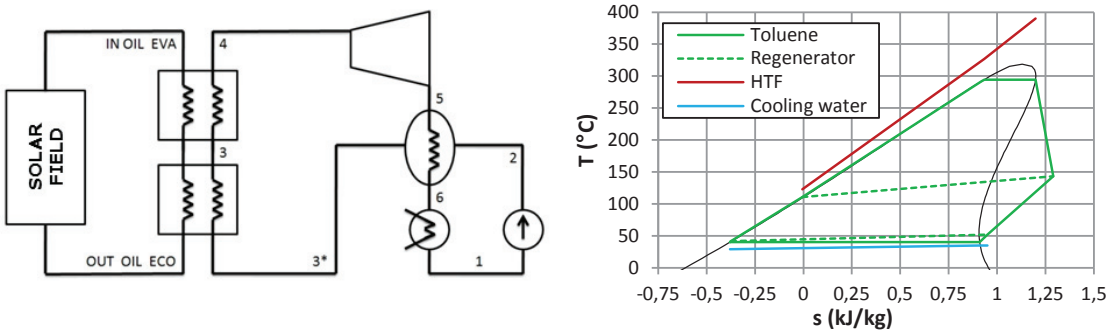

Fig. 1. (Left) Schematic layout of the solar ORC plant and (Right) ORC cycle in the T-s diagram.

With this simplified approach a screening of all different organic fluids available in REFPROP® was firstly performed for different evaporating pressures, in order to identify the fluid that guarantees the highest performance. Once the fluid was selected, the ORC turbine design and performances are studied with an in-house code (Axtur).

The sizing of the heat exchangers is performed in Aspen Exchanger Design & Rating (Aspen EDR® [13]) and the SF piping is sized in Excel® to evaluate the required pumping power and the overall SF aperture area. Sevilla (Spain) is the selected site for the yearly analysis. With the variation of the Effective DNI (EDNI [14]), two different turbine control strategies are compared, namely partial admission and sliding pressure. The turbine control strategy also influences the performance of the other power block (PB) components and of the SF. The off-design behavior of each component is modeled through a set of equations that are solved for every EDNI within the developed Excel spreadsheet. The total plant cost is finally computed as sum of the single equipment costs considering a proper balance of plant taking into account engineering, construction, fine-tuning of the system and performance test costs, while LCOE is computed for both cases.

3. Plant sizing

3.1. Cycle configuration and fluid selection

For a specific selected collector several cycles with different working fluids and maximum temperature were investigated and compared in terms of nominal solar-to-electric efficiency. For this initial screening a constant turbine isentropic efficiency is assumed and the parasitic losses in the solar field are neglected; the set of assumptions used in this first investigation is reported in Table 1.

Table 1. Main assumptions for the ORC plant modelling.

Main Assumptions		
	HT Case	LT case
Solar Field		
Solar multiple	1.2	1.2
Heat Transfer Fluid	Therminol VP1	Therminol 55
HTF maximum temperature (°C)	390	310
Collector type	PT - Eurotrough 100	LFR - SoltiguaFLT10v-24
Collector nominal optical efficiency [0.95 cleanliness factor]	76 %	63.65 %
Power Block		
Cycle net power	5 MW	
Condensing Temperature (°C)	40°C	
ΔT Subcooling at the evaporator inlet (°C)	3°C	
Minimum ΔT at the evaporator or at the economizer (°C)	8°C	
Regenerator efficiency	0.90	
Working fluid liquid side overall pressure drop	0.2 p_{max}	
Working fluid vapor side overall pressure drop	0.05 p_{min}	
Turbine isentropic efficiency	0.80	
Turbine mechanical efficiency	0.99	
Alternator electric efficiency	0.975	
Pump hydraulic efficiency ($\eta_{hydr,pump\_nom}$)	70 %	
Pump motor mechanical/electrical efficiency	90 %	
Wet cooling tower auxiliaries consumption	1.5% Q_{cond}	
Cycle auxiliaries consumption	1% $W_{turb,gross}$	

In order to limit the number of organic fluid to be investigated, a series of constraints was adopted. In particular among all the fluids available in REFPROP only the fluids fulfilling the following characteristics were selected:

- A critical temperature above 200°C to avoid strong heat degradation;
- Saturation pressure at the selected condensing temperature greater than 0.07 bar to avoid strong

depressurization in the condenser;
- Retrograde saturated vapor curve in order to guarantee a superheated vapor dry expansion;
- Reduced variation of the volume ratio ($V_R = \dot{V}_{out,TV}/\dot{V}_{in,TV}$) across the vapor turbine in order to limit the turbine cost. A maximum number of 3 stages is assumed and a maximum variation of volume across the overall turbine of 1000 (10 per stage) was assumed to limit design penalties. Not knowing the best evaporation pressure for each fluid, this ratio was computed assuming saturated vapor at temperature 20 degrees below the critical temperature and assuming an isentropic expansion down to the condensing pressure.

In Fig. 2, Left are reported the Andrews curves for the 9 organic fluids that fulfill the abovementioned requirements, while in Fig. 2, Right is reported the nominal solar-to-electric efficiency as a function of the evaporation temperature of different solar ORC cycles using ET-100 collectors: due to the use of high temperature designed collector, there is no penalty in increasing the working temperature and the predominant effect is the cycle efficiency increase.

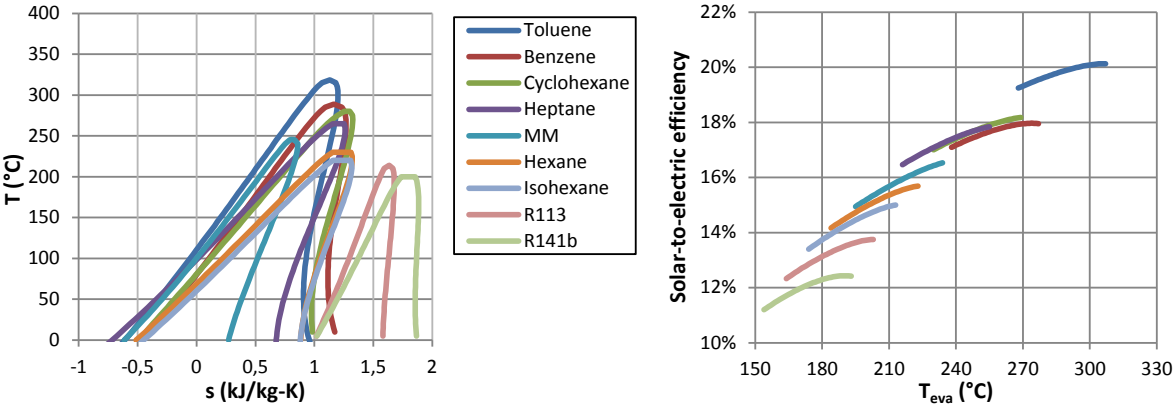

Fig. 2. (Left) Andrews curves for the 9 selected organic fluids and (Right) nominal solar-to-electric efficiency as a function of the evaporation temperature for the 9 selected fluids (HT case).

Based on this preliminary analysis, Toluene was selected as working fluid in the following analysis. With the same approach Toluene was assumed as the best option also for a solar field adopting low temperature collectors.

3.2. Detailed analysis with axial turbine design and solar field sizing

The initial screening presented in section 3.1 required a series of simplifying hypotheses that can now be removed to improve the whole system simulation. A parametric analysis of the effect of the evaporation pressure variation on the solar-to-electric efficiency is now performed estimating for every evaporation pressure the turbine isentropic efficiency ($\eta_{is,TV}$) with an in-house code named Axtur [15]. The software requires as input data the turbine inlet conditions (temperature T, pressure p, mass flow $\dot{m}$ and working fluid type), the expansion ratio and the desired number of stages. Then the code performs an optimization of the turbine geometry in order to maximize the isentropic efficiency for a given rotational speed, solving the mass and energy balances and applying the loss model developed by Craig & Cox for axial turbines [16].The code output provides the user with all geometric information (number of blades, blades height and orientation etc.) about the designed machine, the thermodynamic conditions and velocities at each stage inlet, the degree of reaction and the turbine isentropic efficiency.

The turbine isentropic efficiency affects the turbine outlet conditions and consequently the cycle efficiency, making the design process iterative: a first guess isentropic efficiency is used to solve the thermodynamic cycle and the obtained mass flow is used as Axtur input for a first sizing; the process is stopped when the difference in turbine isentropic efficiency between two iterations is below a chosen target. Both for the HT and LT cases, a three stages

axial turbine was selected: the choice of a three stages machine is justified by the value of volume ratio across the vapor turbine above 1000. In order to have a proper design of the first stage where the volumetric flow is particularly low, a partial admission solution is the suggested option by Axtur. The trends of the isentropic efficiency, the volume ratio and the admission degree as a function of the evaporation temperature obtained with Axtur are reported in Fig. 3 Left, both for the LT and HT case. Both machines are sized assuming 3000 rpm as rotational speed, avoiding the use of a gear box, thus limiting the PB costs.

In order to have a reliable estimate of the solar field parasitic consumption, for each evaporation temperature a sizing of the solar field was required. For each evaporative pressure the HTF velocity in the SF piping system and in the collectors was optimized minimizing the annual piping cost ($C_{pip,y}$) computed as follows:

$$C_{pip,y} = C_{pumping,y} + C_{Q_{loss},y} + FCR \cdot (C_{met} + C_{ins} + C_{fitt} + C_{supp} + C_{pump} + C_{install}) \quad (1)$$

The operational costs, taking into account the yearly cost related to the thermal losses ($C_{Q_{loss},y}$) and the yearly pumping electric consumption costs ($C_{pump,y}$), are computed as:

$$C_{Q_{loss},y} = \dot{Q}_{loss,nom} \cdot n \cdot \eta_{PB+Aux\_eq} \cdot c_{EE} \quad (2)$$

$$C_{pump,y} = \left(W_{pump,design} \cdot \sum_{i=1}^{n} \left(\frac{\dot{m}_i}{\dot{m}_{nom}} \right)^3 \cdot \frac{\eta_{hydr,pump\_nom}}{\eta_{hydr,pump\_i}} \right) \cdot c_{EE} \quad (3)$$

where $\dot{Q}_{loss,nom}$ are the piping thermal losses, n is the number of operating hours, η_{PB+Aux_eq} is the equivalent yearly efficiency with whom the thermal energy is converted into electric energy and c_{EE} is the electric energy cost.

Through the Fixed-Charge Rate (FCR) method [17] the piping investment cost, computed as sum of the piping metal cost (C_{met}), the insulating material cost (C_{ins}), the fittings cost (C_{fitt}), the tube supports cost (C_{supp}), the SF pump cost (C_{pump}) and the piping installation cost ($C_{install}$), is distributed over the total plant life. The FCR is defined as the fraction of the investment cost that the investor has to cover every year to face the yearly depreciation or return of the capital, tax expense, and insurance expense associated with the installation of a specific generating unit for the utility or company involved.

The solar-to-electric efficiency trend as a function of the evaporative temperature for the two considered plants is finally reported in Fig. 3, Right: each point of the curve corresponds to an optimized solar field that minimizes, for the chosen evaporative pressure, the yearly piping costs.

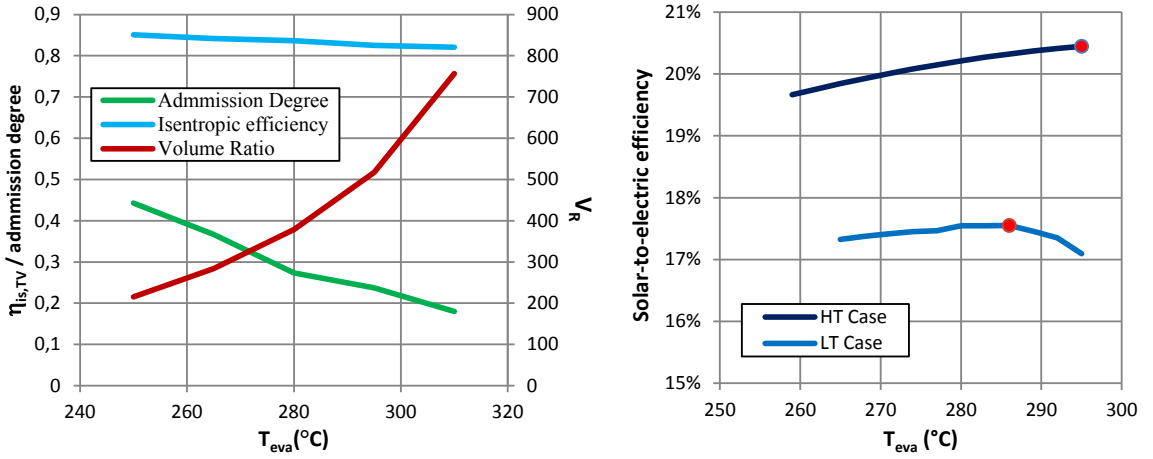

Fig. 3. (Left) Toluene turbine isentropic efficiency, volume ratio and admission degree as a function of the turbine inlet temperature for the HT and LT cases. (Right) Solar –to-electric efficiency for the HT and LT solar field case as a function of the evaporation pressure

For the plant implementing Soltigua collectors, the maximum solar-to-electric efficiency was obtained for an evaporation pressure corresponding to 286°C, while in the HT case the best efficiency coincides with the maximum investigated temperature (295°C) whose value was assumed equal to the critical temperature minus a safety margin to guarantee a dry vapor expansion. For the two best cases a further investigation was performed: the primary heat exchangers and the condenser were sized with Aspen EDR®, while the regenerator was sized with proprietary software developed by LUVE, allowing a more precise estimate of the exchangers pressure drops. Main results for the two cases scoring the highest solar-to-electric efficiency are reported in Table 2; results differ slightly from the ones presented in Fig. 3, due to the adjustment of the cycle pressure losses according to the value obtained in the heat exchangers sizing phase. The T-s diagrams of LT and HT cases are finally reported in Fig. 4.

Table 2. Main design results for the two best cases (LT and HT).

	HT case	LT case
Solar Field		
Solar Field HTF outlet temperature (°C)	390	310
Solar Field inlet temperature (°C)	119.3	255.7
HTF mass flow(kg/s)	29.44	114.23
Solar field efficiency	74.6%	62.6%
Solar field aperture area (m^2)	35230	42182
Power Cycle		
Evaporation temperature (°C)	295	286
Working fluid mass flow(kg/s)	29.3	29.6
Cycle thermal input (kW)	17511	17614
Turbine volume ratio	483	392
Turbine isentropic efficiency	83.3%	83.7%
Cycle efficiency	28.55%	28.4%
Solar to electric efficiency	20.4%	16.7%

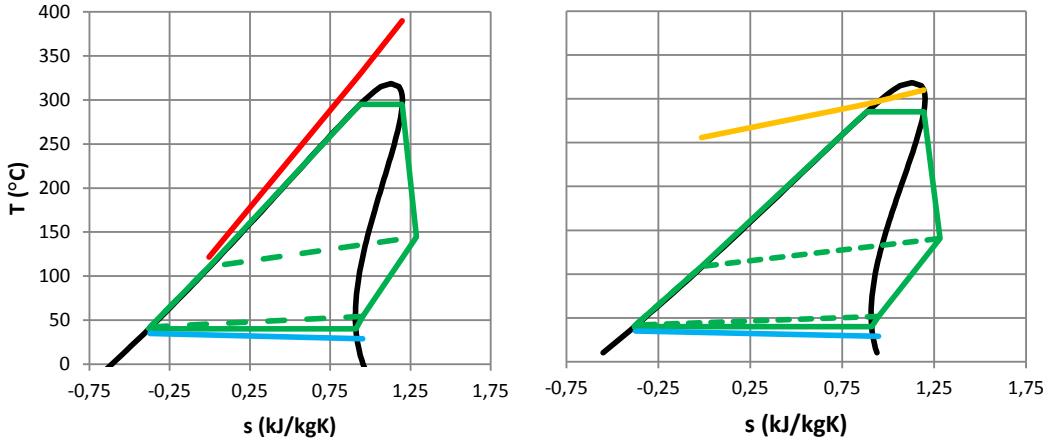

Fig. 4. T-s diagram of the optimum cycle for the HT case (Left) and LT case (Right). HTF curves are qualitatively reported with red and yellow curves, respectively for HT and LT case.

4. Off design simulation

Due to the lack of storage system, the electric production of the ORC cycle is directly affected by the available solar radiation. In order to perform a simplified yearly analysis the only DNI variation effect was considered, neglecting the effect of the ambient temperature variation, which is considered secondary due to the chosen condensing system (WCT). The off-design behavior of each plant component was described by a set of equations and the whole equations system was solved within Excel giving the new cycle working conditions (thermodynamic conditions in every cycle point and whole cycle performance) as output. For every value of the Effective DNI, it was thus possible to evaluate the whole cycle performance.

4.1. Solar field

In order to express the PB performance as a function of the solar radiation it was computed its effective value for every hour of the year. The effective solar radiation, whose definition has been already introduced in previous works [14], can be computed for PT and LFR collectors respectively as:

$$EDNI_{PT} = DNI \cdot K(\theta)_{PT} \cdot \eta_{shadowing} \cdot \eta_{end\_loss} \tag{4}$$

$$EDNI_{LFR} = DNI \cdot IAM_{long}(\theta_i) \cdot IAM_{tr}(\theta_{tr}) \cdot \eta_{end\_loss} \tag{5}$$

The hourly values of DNI for Seville (Spain, $\phi_{LAT} = 37.42°, \phi_{LONG} = -5.9°, STZ = 1$) are obtained from [18], while the incidence angles on the collector and the value of end losses and shading between parallel rows were computed with the set of equations presented in [14]. Finally, the values of $K(\theta)$ for the ET-100 collector and the two IAM for the Soltigua FLT10v-24 LFR are given in [14] and [9] respectively. In Fig. 5 the DNI values for Seville and the obtained EDNI for the PT and LFR collectors are reported. It is possible to see how the presence of two incidence angles reduces the effective radiation available at the LFR collector aperture.

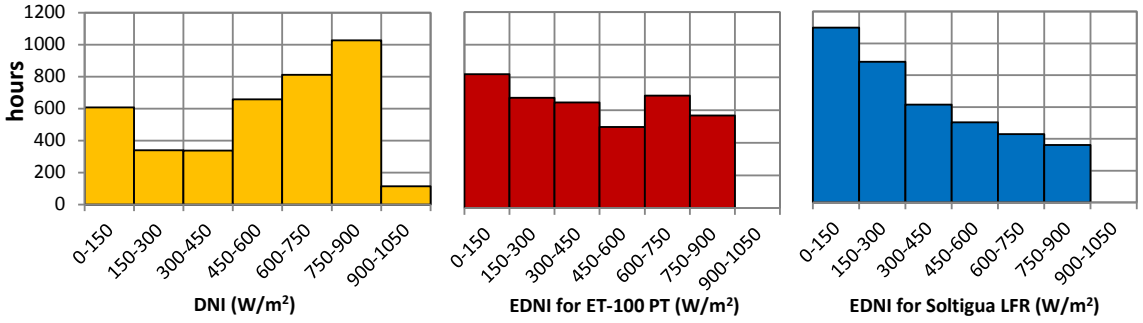

Fig. 5. (Left) DNI trend for Seville and EDNI for the HT (Centre) and LT (Right) solar field.

The solar field HTF outlet temperature was kept constant for any value of $EDNI$ and for simplicity the collector thermal losses were supposed only function of the HTF average temperature, neglecting the influence of the $EDNI$. The piping system thermal losses were kept constant.

4.2. Power block

The reduction of power cycle thermal input with the solar radiation implies a reduction of the working fluid mass flow and thus a variation of the turbine performance. In the present work two different control strategies for the vapor turbine were investigated:

- Sliding pressure: the turbine inlet pressure decreases proportionally to the reduction of turbine inlet mass flow;
- Partial admission: the turbine inlet pressure is kept constant in off-design conditions varying the turbine inlet area; this is obtained reducing the area of annulus where the fluid is fed, through inlet guide vanes on the first stage stator. The remaining turbine stages work in sliding pressure.

In both cases a correction of the turbine isentropic efficiency has to be performed: turbine isentropic efficiency was changed as a function of the ratio between the actual enthalpy drop and the design enthalpy drop, as proposed in [19]. This correlation was applied to the whole vapor turbine in sliding pressure and to each turbine stage in the partial admission case. The obtained turbine isentropic efficiency as a function of the cycle thermal input is reported in Fig. 6.

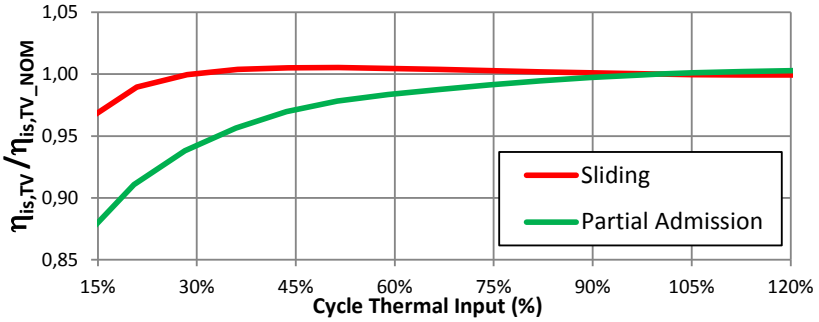

Fig. 6. Turbine isentropic efficiency as a function of the power cycle thermal input for both operating strategies.

Both power cycle and solar field pumps off design hydraulic efficiencies were computed as a function of the ratio between the actual and nominal mass flow coefficient $\varphi/\varphi_{nom,pump}$, assuming a variable speed drive. The pump hydraulic efficiency correction curve, reported in Fig. 7, Left, was obtained from Thermoflex 23® [20], as well as the pump motor mechanical/electrical efficiency, the turbine shaft losses and the alternator efficiency off design curves, all reported in Fig. 7, Right.

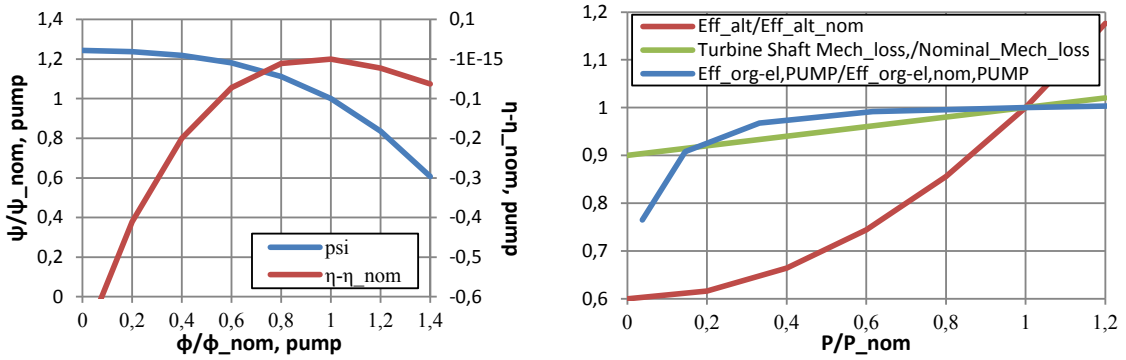

Fig. 7. (Left) Pump hydraulic efficiency and load coefficient as function of the mass flow coefficient; (Right) pump motor mechanical/electrical efficiency, turbine shaft losses and the alternator efficiency as a function of the dimensionless load.

The pressure drops in the heat exchangers were corrected proportionally to V^2, assuming a completely turbulent flow in the heat exchangers tube, while their overall heat transfer coefficient U was corrected assuming:

$$(UA)_{off} = (UA)_{design}\left(\frac{\dot{m}_{off}}{\dot{m}_{design}}\right)^{n} \tag{6}$$

where n, if the thermal conductivity resistance of the heat exchanger tube walls is neglected, depends only on the variation of both the internal (h_{in}) and external (h_{out}) convection heat transfer coefficients. If the Nu_{in} number is computed with the Dittus-Boelter correlation and Nu_{out} with the Zukauskas correlation their value is proportional to $v^{0.8}$ and $v^{0.63}$, respectively [21]. An intermediate value of n equal to 0.7 was therefore assumed in (6).

Finally, for the wet cooling tower off-design behavior, the water tower temperature was kept constant, while the tower electric consumptions (fan and tower circulating pump) were assumed proportional to the heat rejected at the cycle condenser (down to the 20% of the nominal consumption, below this value they are assumed constant).

The whole cycle performance is obtained solving the above system of equations above mentioned for a given EDNI value. The overall cycle performance as function of the adimensional EDNI obtained with the off design simulation is reported in Fig. 8 for the HT case and for the two different turbine control strategies.

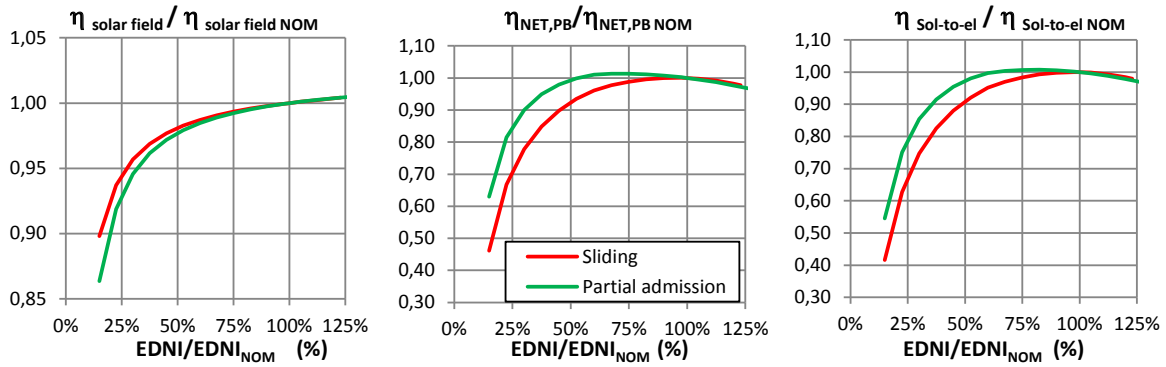

Fig. 8. Solar field efficiency (left), power block efficiency (centre) and cycle performance variation (right) as function of the adimensional for the HT case: sliding pressure and partial admission cases are reported.

5. Yearly energy yield and LCOE

In Table 3 the yearly results for the different cases are reported: the case allowing the highest yearly energy yield is the HT case with partial admission. The better SF yearly performance of the HT case is mainly due to the choice of PT collectors that have higher nominal optical efficiency and are less penalized in off design conditions with respect to LFR used in the LT case (see Fig. 5); in addition the higher evaporation temperature guarantees also higher power block efficiencies with respect to the LT case.

Considering the control strategy, partial admission leads to better results for both LT and HT cases: although in sliding pressure the solar field thermal performance are better due to the reduction of the SF inlet temperature with the DNI, this effect doesn't counterbalance the lower cycle performance obtained with sliding pressure leading to overall higher performance of the partial admission control strategy. In the LT case the lower SF yearly optical efficiency with sliding pressure control is due to a strong increase of the HTF mass flow for high DNI values that causes the system to defocus to avoid circulating pumps overload (see also HTF curves in Fig. 4 Right).

Table 3. Yearly results for the LT and HT cases and for two different turbine control strategies.

	HT case			LT case		
	Sliding pressure	Partial admission	Design	Sliding pressure	Partial admission	Design
η_{opt}	58.2%	58.3%	76.0%	38.5%	39.9%	63.7%
η_{th}	97.1%	96.9%	98.0%	97.4%	97.0%	98.4%
η_{th_piping}	99.7%	99.7%	99.8%	99.1%	99.1%	99.5%
η_{net_PB}	26.4%	27.1%	27.5%	26.1%	26.8%	27.3%
η_{AUX_SF}	99.6%	99.6%	99.4%	98.7%	98.2%	97.9
$\eta_{solar\ to\ electric}$	14.8%	15.2%	20.4%	9.6%	10.1%	16.7%
Electric Energy (MWh)	10894	11203		8436	8912	

The LCOE was evaluated for the HT case, while for the LT case it was calculated the specific solar field cost necessary to obtain the same LCOE of the best HT case (partial admission). First of all it was necessary to estimate the overall plants cost: the primary heat exchangers and the condenser costs were obtained in the sizing phase with Aspen EDR®, the pumps and WCT costs were estimated with Thermoflex, while the regenerator cost and the turbine cost were estimated with the correlations proposed in [22]:

$$C_{rig}\ [€] = 450000 \cdot \left(\frac{A}{1000}\right)^{0.7} \tag{7}$$

$$C_{turb}[€] = 240'000 \cdot \left(W_{turb,gross}\right)^{0.99} + 61'750 \cdot \left(\frac{SP}{0.18}\right)^{1.06} \cdot (n_{st})^{1.18} \tag{8}$$

where $W_{turb,gross}$ is the turbine gross power, n_{st} is the turbine number of stages and SP is the turbine Size Parameter[†].

The BOP cost was assumed equal to 69% of the overall power block cost and the solar field cost for the HT case was assumed equal to 220 €/m^2 as suggested in [14]. The other assumptions used to compute the LCOE are reported in Table 4.

Table 4. Main economic assumptions for the LCOE cost calculation.

Indirect Costs (% of total estimated cost)	14%
Owner & contingencies (% of total estimated cost)	15%
O&M Costs (% of total plant cost)	1.5%
Debt (%)-Equity shares	60%-40%
Interests on Debt – Interests on Equity (%)	5%-13%
Plant life (years)	25

Table 5. Main economic results.

		HT case	LT case (Partial Admission)
Total solar field Cost	**€**	**7'960'470**	**5'492'973'9**
Collectors		*7'750'556*	*5'017'459*
Piping		*199'108*	*403'792*
Oil pump		*10'806*	*71'724*
PB+BOP cost	**€**	**4'497'975**	**4'417'440**
Economizer		*191'506*	*71'765*
Evaporator		*33'789*	*108'042*
Turbine		*1'437'911*	*1'451'913*
Feed pump		*93'501*	*86'466*
Wet Cooling Tower pump		*58'906*	*59'308*
Condenser		*210'914*	*207'276*
Wet Cooling Tower		*512'892*	*516'094*
Regenerator		*122'103*	*122'153*
BOP		*1'836'451*	*1'809'882*
TOTAL ESTIMATED COST	**€**	**12'458'446**	**9'910'415**
TOTAL PLANT COST	**€**	**16'333'022**	**12'992'554**
ANNUAL O&M COST	**€**	**244'995**	**194'888**
Annual energy yield Partial admission (MWh)		11203	8912
Annual energy yield Sliding pressure (MWh)		10894	
LCOE Partial Admission (€/MWh)		**175.39**	**175.39**
LCOE Sliding Pressure (€/MWh)		**180.36**	
Estimated collector cost (€/m^2), partial admission		**220.0**	**119.0**

LCOE for HT case is about 180 €/MWh with partial admission and 175 €/MWh with sliding pressure off-design control strategy. LCOE for LT Fresnel based plants reaches the same values as parabolic trough case when its specific cost is about half than the parabolic trough collector. This occurrence is similar to what is found in literature for large scale CSP plants [14].

6. Conclusions

The performances of a 5MW$_{el}$ ORC cycle coupled with two types of linear collectors have been evaluated. The solar collectors are respectively parabolic trough collectors with synthetic oil Therminol VP1 and a maximum temperature of 390°C (HT), and Fresnel reflectors with Therminol 55, limited to an operating temperature of 310°C (LT). The working fluid Toluene has been selected for both cases by means of a preliminary simplified

[†] The size parameter of a turbine is defined as $SP = \frac{\sqrt{\dot{V}_{out}}}{\sqrt[4]{\Delta h_{is}}}$

optimization. An in-house code has been developed for off-design calculation of the whole system, which enabled the comparison of two different control strategies for the plant, respectively sliding pressure and a fixed pressure at the turbine inlet. The latter is obtained through a partial admission of the turbine and, both for HT and LT collectors, it leads to higher electricity outputs. In fact, in this case the higher power block efficiency overcomes the effect of a decrease in solar field efficiency, due to average HTF temperatures that are kept high within the solar field. For a specific site (Sevilla, Spain) the yearly solar-to-electric efficiencies for HT case with partial admission and sliding operation are respectively 15.2% and 14.8%. Sliding pressure penalty is even more evident with LT Fresnel collectors, as defocusing may occur during operation with high DNI values. In fact, these irradiance would cause a very high increase of HTF mass flow rate, bringing to an overload of the circulating pumps (efficiency is respectively 10.1% and 9.6%). LCOE is finally computed for HT case with both control strategies, resulting about 180 €/MWh with partial admission and 175 €/MWh with sliding pressure off-design control strategy. LCOE for Fresnel based plants would reach the same values as parabolic trough case when its specific cost is about half than the parabolic trough collector. It has to be noticed that sliding pressure mode is easy to implement in an actual plant and leads to a self-adjusting and reliable operation, while partial admission should generate some increase in the turbine cost that has been neglected in this analysis. Future works should examine in depth this aspect, together with the exploitation of superheated ORC cycles for HT applications, the insertion of a thermal storage and possibly the case of cogenerative systems.

References

[1] Bombarda P., Astolfi M., Silva P., “Estimating cost of the geothermal power technologies”, Proceedings of Geopower Europe, December 2011, Milano
[2] Obernberger, I., Gaia, M., 2005. Biomass-Power-Heat Coupling Based on the ORC Process – State-of-the-art and Possibilities for Process Optimization. VDI Berichte, 131–148.
[3] Invernizzi, C., Iora, P., Silva, P., 2007. Bottoming micro-Rankine cycles for micro-gas turbines. Applied Thermal Engineering 27, 100–110.
[4] Hung T.C., Shai T.Y., Wang S.K., A review of organic rankine cycles (ORCs) for the recovery of low-grade waste heat, Energy, 1997, Volume 22, Issue 7, 661-667.
[5] Prabhu, E., 2006. Solar Trough Organic Rankine Electricity System (STORES) Stage 1: Power Plant Optimization and Economics. Technical Report NREL/SR-550-39433 National Renewable Energy Laboratory.
[6] Canada, S., Brosseau, D., Price, H., 2006. Design and construction of the APS 1-MWE parabolic trough power plant. In: Proceedings of the ASME International Solar Energy Conference 2006, vol. 2006. Denver, CO.
[7] Geyer M, Lüpfert E, Osuna R, Esteban A, Schiel W, Schweitzer A, et al. EUROTROUGH-Parabolic trough collector developed for cost efficient solar power generation 2002:04-06.
[8] Solutia. Therminol VP1 vapour phase liquid phase heat transfer fluid; 2014.
[9] Soltigua. Concentratore Lineare Fresnel - Scheda Tecnica 2014.
[10] Solutia. Therminol 55 Efficient, reliable, synthetic heat transfer fluid; 2014.
[11] Turboden. Turbogeneratori ORC: soluzioni per impianti solari termodinamici di piccola taglia. SolarExpo, May 2013, Milano, Italy.
[12] Lemmon EW, Huber ML, McLinden MO. NIST reference fluid thermodynamic and transport properties–REFPROP 2002.
[13] AspenTech. Aspen Exchanger Design & Rating; 2014.
[14] Giostri A, Binotti M, Silva P, Macchi E, Manzolini G. Comparison of two linear collectors in solar thermal plants: Parabolic trough versus Fresnel. Journal of Solar Energy Engineering, Transactions of the ASME 2013;135.
[15] Macchi E, Perdichizzi A. Efficiency Prediction for Axial-Flow Turbines Operating with Nonconventional Fluids. Journal of engineering for power 1981;103:718-724.
[16] Craig H, Cox H. Performance estimation of axial flow turbines. Proceedings of the Institution of Mechanical Engineers 1970;185:407-424.
[17] Short W, Packey DJ, Holt T. A Manual for the Economic Evaluation of Energy Efficiency and Renewable Energy Technologies University Press of the Pacific; 2005.
[18] U.S. Department of Energy. EnergyPlus Energy Simulation Software - Weather data; 2014.
[19] Macchi E, Perdichizzi A. Theoretical Prediction of the Off-Design Performance of Axial-Flow Turbines:1867-1896.
[20] Thermoflow. Thermoflex: Fully-flexible design and simulation of combined cycles, cogeneration systems, and other thermal power systems;2014.
[21] Incropera FP. Fundamentals of Heat and Mass Transfer John Wiley & Sons; 2011.
[22] Astolfi M. An innovative approach for the techno-economic optimization of organic Rankine cycles 2014.